Supplementary Information

Thermo-sensitive poly(L-methionine) hydrogel facilitates regenerative repair of diabetic wounds by modulating immune microenvironments

Mengtian Xie,[a,b] Yirong Sun[a] and Jianxun Ding*[a,b]

[a]*State Key Laboratory of Polymer Science and Technology, Changchun Institute of Applied Chemistry, Chinese Academy of Sciences, 5625 Renmin Street, Changchun 130022, P. R. China. E-mail: jxding@ciac.ac.cn*

[b]*School of Applied Chemistry and Engineering, University of Science and Technology of China, 96 Jinzhai Road, Hefei 230026, P. R. China*

Experimental section

Regents and materials

Methoxy poly(ethylene glycol) (mPEG; number-average molecular weight (M_n) = 2000 g mol^{-1}), tetrahydrofuran (THF), *N,N*-dimethylformamide (DMF), and dichloromethane (DCM) were purchased from Energy Chemical (Anhui, P. R. China). L-Norleucine (L-Nle) and L-methionine (L-Met) were bought from Aladdin (Shanghai, P. R. China). Deuterated chloroform ($CDCl_3$), deuterated trifluoroacetic acid (TFA-*d*), and deuteroxide (D_2O) were supplied from Cambridge Isotope Laboratories, Inc. (Andover, MA, USA). Triphosgene was obtained from Macklin Biochemical Co., Ltd. (Shanghai, P. R. China). Hydrogen peroxide (H_2O_2), lipopolysaccharide (LPS), and streptozotocin (STZ) were obtained from Sigma-Aldrich (Shanghai, P. R. China). 1,1-Diphenyl-2-picrylhydrazyl (DPPH) and 2,2'-azinobis-(3-ethylbenzothiazoline-6-sulfonic acid) (ABTS) assay were obtained from Nanjing Jiancheng Bioengineering Institute (Nanjing, P. R. China). All other chemical reagents and solvents were purchased from Sinopharm Chemical Reagent Co., Ltd. (Shanghai, P. R. China) and used as received.

HaCaT cells and RAW 264.7 cells, phosphate-buffered solution (PBS), Dulbecco's modified Eagle's medium (DMEM), penicillin/streptomycin liquid, Live/Dead staining kit, Annexin V-FITC/propidium iodide (PI) apoptosis detection kit, and dichlorofluorescein diacetate (DCFH-DA) staining kit were sourced from Servicebio Technology Co., Ltd. (Wuhan, P. R. China). L929 cells were obtained from Saiwen Innovation Biotechnology Co., Ltd. (Beijing, P. R. China). Fetal bovine serum (FBS) was bought from Gibco (Grand Island, NY, USA). Cell Counting Kit-8 (CCK-8) was purchased from Heyuan Liji Biotechnology Co., Ltd. (Shanghai, P. R. China). Zombie Aquera, allophycocyanin-F4/80 (APC-F4/80), Super Bright 645-CD80 (SB645-CD80), phycoerthrin-CD206 (PE-CD206), Mouse IL-6 Uncoated enzyme-linked immunosorbent assay (ELISA) kit, Mouse TNF-α Uncoated ELISA kit, Mouse IL-10 Uncoated ELISA kit, and Human/Mouse TGF-β1 Uncoated ELISA kit were purchased from Thermo Fisher Scientific (Waltham, MA, USA). Male C57BL/6N mice (4−5

weeks, SPF) were procured from Charles River Laboratories (Beijing, P. R. China). All animals met specific pathogen-free standards and had not undergone any prior drug treatment or experimental procedures.

All animal procedures were performed in accordance with the Guidelines for Care and Use of Laboratory Animals of Changchun Institute of Applied Chemistry, Chinese Academy of Sciences, and approved by the Animal Ethics Committee of IACUC Issue No. CIAC 2021[0023].

Synthesis and characterizations of amino-terminated methoxy poly(ethylene glycol)

mPEG (25.0 g, 12.5 mmol), tosyl chloride (9.5 g, 50.0 mmol), and potassium hydroxide (5.6 g, 100.0 mmol) were dissolved in DCM (250.0 mL) and stirred at room temperature for nine days. The mixture was then washed with ice-cold saturated sodium chloride (NaCl) solution and dried over magnesium sulfate ($MgSO_4$). After filtration and rotary evaporation, the residue was precipitated in ice-cold diethyl ether, collected by suction filtration, and vacuum-dried at room temperature. The obtained intermediate was dissolved entirely in aqueous ammonia (250.0 mL), followed by the addition of an equal mass of ammonium chloride under stirring. The mixture was allowed to react at room temperature for seven days. The organic phase was extracted with DCM, washed with ice-cold saturated NaCl solution, and dried over anhydrous $MgSO_4$. The following day, after filtration, the product was precipitated with ice-cold diethyl ether, filtered, and vacuum-dried to obtain the final product methoxy poly(ethylene glycol) amine (mPEG-NH_2, 18.2 g, yield: 72%). The structures of mPEG and mPEG-NH_2 were confirmed by carbon-13 nuclear magnetic resonance carbon spectroscopy (^{13}C NMR) using $CDCl_3$ as the solvent.

Synthesis and characterizations of L-norleucine *N*-carboxyanhydride

L-Nle (15.0 g, 0.114 mol) and bis(trichloromethyl) carbonate (BTC; 17.0 g, 0.057 mol) were dispersed in anhydrous THF (300.0 mL) in a dry three-necked flask under a nitrogen (N_2) atmosphere. The reaction was maintained at 52 °C for 2 h until the solution became clear. The reaction solution was then cooled to room temperature and concentrated. The crude product was precipitated with ice-cold *n*-hexane, collected by suction filtration, and dissolved in ethyl acetate. Subsequently, the organic phase was washed three times with saturated NaCl solution, dried over anhydrous $MgSO_4$, and stored at −20 °C overnight. $MgSO_4$ was removed the next day. Finally, the solvent was removed under vacuum to yield pure L-norleucine *N*-carboxyanhydride (L-Nle NCA; 9.3 g, 51.8% yield). Nle NCA was characterized by proton nuclear magnetic resonance (^1H NMR) using $CDCl_3$ as the solvent.

Synthesis and characterizations of L-methionine *N*-carboxyanhydride

L-Met (20.0 g, 0.134 mol) and BTC (20.0 g, 0.067 mol) were dispersed in anhydrous THF (300.0 mL) in a dry three-necked flask under a N_2 atmosphere. The reaction was conducted at 48 °C for 1 h until the solution became clear. The solution was then cooled to room temperature and concentrated. The crude product was precipitated with ice-cold *n*-hexane, decanted from the upper layer, and dissolved in ethyl acetate. The organic layer was washed three times with saturated NaCl solution, dried over anhydrous $MgSO_4$, and stored at −20 °C overnight. $MgSO_4$ was removed the next day. Finally, pure L-methionine *N*-carboxyanhydride (L-Met NCA; 9.6 g, yield: 40.9%) was obtained by moving the solvent under vacuum. ^{1}H NMR confirmed the structure of Met NCA in $CDCl_3$.

Synthesis and characterizations of methoxy poly(ethylene glycol)-*block*-poly(L-norleucine)

mPEG-NH_2 (1.00 g, 0.5 mmol) was dissolved in toluene (150.0 mL) and subjected to azeotropic dehydration at 125 °C for 2 h. After cooling to room temperature, anhydrous DMF (40.0 mL) and L-Nle NCA (1.96 g, 12.5 mmol) were added, and the reaction proceeded at room temperature for 72 h under a N_2 atmosphere. Subsequently, the product was precipitated in ice-cold diethyl ether, centrifuged at 8000 rpm for 3 min, and the supernatant discarded. The precipitate was redissolved in DMF, and the purification cycle was repeated three times. The purified product was then transferred into a dialysis bag (molecular weight cut-off (MWCO) = 2000 Da) and dialyzed against deionized water for three days, followed by lyophilization to yield a white, powdery solid of methoxy poly(ethylene glycol)-*block*-poly(norleucine) ($EG_{45}Nle_{25}$; 1.05 g, yield: 43.5%). $EG_{45}Nle_{25}$ was characterized by Fourier-transform infrared spectrum (FT-IR) and ^{1}H NMR spectroscopy using TFA-*d* as the solvent.

Synthesis and characterizations of methoxy poly(ethylene glycol)-*block*-poly(L-methionine)

mPEG-NH_2 (1.00 g, 0.5 mmol) was dissolved in toluene (150.0 mL), followed by azeotropic dehydration at 125 °C for 2 h. Then, anhydrous DMF (40.0 mL) and L-Met NCA (2.19 g, 12.5 mmol) were added, and the mixture was stirred at room temperature for 72 h under a N_2 atmosphere. Subsequently, the product was precipitated in ice-cold diethyl ether, centrifuged at 8000 rpm for 3 min, and the supernatant was discarded. The precipitate was redissolved in DMF, and this purification cycle was repeated three times. The product was then transferred into a dialysis bag (MWCO = 2000 Da) and dialyzed against deionized water for three days, followed by lyophilization to yield a white, powdery solid, methoxy-poly(ethylene glycol)-*block*-poly(methionine) ($EG_{45}Met_{25}$; 1.17g, yield: 44.3%). The structure of $EG_{45}Met_{25}$ was confirmed by ^{1}H NMR and FT-IR using TFA-*d* as a solvent.

Sol-to-gel transition measurement

Solutions with varying concentrations (8.0, 10.0, 12.0, 14.0, and 16.0 mmol L^{-1}) were prepared in PBS and stirred in an ice-water bath for 72 h. The temperature was then increased from 4 °C in 1 °C increments, maintaining each temperature for 5 min to ensure stabilization. Gelation kinetics were evaluated using the inverted-vial assay, where a complete sol-to-gel transition was defined as the absence of flow for over 30 s upon inversion.

Rheological measurements

Solutions were prepared in PBS and stirred in an ice-water bath for 72 h. Rheological measurements were conducted using a parallel-plate geometry (Diameter: 25.0 mm; Gap: 0.5 mm) under oscillatory shear on an MCR 301 rheometer (Anton Paar, Graz, Austria). A temperature sweep was performed from 4 to 50 °C at a heating rate of 0.5 °C min^{-1}, with an angular frequency of 1.0 rad s^{-1} and a strain amplitude of 1.0%. The storage modulus (G') and loss modulus (G'') were recorded to assess the viscoelastic behavior of the hydrogel.

Secondary structure analysis

The polymer was dissolved in MilliQ water to prepare a 0.02 mg mL^{-1} solution. Circular dichroism (CD) spectroscopy was conducted on an Applied Photophysics Chirascan Circular Dichroism spectrometer (Applied Photophysics, Shanghai, P. R. China) over the 180−260 nm wavelength range. Temperature-dependent scans were conducted from 10 to 70 °C at 10 °C intervals to monitor thermally induced changes in the polymer's secondary structure.

Cryo-scanning electron microscope (cryo-SEM)

The microstructure of the post-gelation hydrogels was examined by cryo-scanning electron microscopy (FEI XL 30 ESEM FEG; FEI Company, Hillsboro, OR, USA).

Antioxidation capacity of hydrogels

The antioxidant properties of $EG_{45}Met_{25}$ were evaluated using ^1H NMR, CD spectroscopy, DPPH assay, and ABTS assay.

For the reactive oxygen species (ROS)-responsiveness study, $EG_{45}Met_{25}$ (2.0 mg) was dissolved in D_2O (1.0 mL) and stirred in an ice-water bath for 72 h. H_2O_2 was then added to achieve final concentrations of 10.0, 20.0, and 40.0 mmol L^{-1}. The mixtures were incubated at 37 °C in a constant-temperature shaker. Samples were analyzed at 24-h intervals using 300 MHz ^1H NMR spectroscopy (Bruker BioSpin GmbH, Rheinstetten, Germany) to monitor chemical structure changes, and CD spectroscopy to assess secondary structural changes.

The DPPH radical scavenging capacity of $EG_{45}Met_{25}$ was quantified using a commercial assay kit (Nanjing Jiancheng Bioengineering Institute, Nanjing, P. R. China). Serial dilutions of $EG_{45}Met_{25}$ were incubated with the DPPH working solution in the dark at room temperature for 6 min. The absorbance at 517 nm was measured using a JASCO V-770 ultraviolet−visible (UV−Vis) spectrometer (JASCO, Tokyo, Japan). The DPPH radical-scavenging ability was calculated using Equation S1.

$$DPPH\ scavenging\ ratio\ （\%）= \frac{A_{Control} - A_{Sample}}{A_{Control}} \times 100\%$$

S1

Similarly, the ABTS radical scavenging capacity of $EG_{45}Met_{25}$ was evaluated using the same assay provider (Nanjing Jiancheng Bioengineering Institute, Nanjing, P. R. China). Serial dilutions of $EG_{45}Met_{25}$ were incubated with the ABTS working solution in the dark at ambient temperature for 6 min. The absorbance peak at 405 nm was measured using a microplate reader (Bio-Rad; Hercules, CA, USA), and the scavenging ability was calculated as Equation S2.

$$ABTS\ scavenging\ ratio\ （\%）= \frac{A_{Control} - A_{Sample}}{A_{Control}} \times 100\%$$

S2

Biocompatibility of hydrogels

The cytotoxicity of hydrogels toward HaCaT and L929 cells was evaluated using a CCK-8 assay (Heyuan Liji Biotechnology Co., Ltd., Shanghai, P. R. China). Cells were seeded in 96-well plates at a density of 5.0×10^3 cells per well in 100.0 μL complete medium and allowed to adhere for 24 h. The medium was then replaced with fresh medium containing the hydrogel (6.25−400.0 μmol L^{-1}, 10.0 μL per well) or without hydrogel (control). After 24 and 72 h of incubation, cell viability was determined using the CCK-8 assay according to the manufacturer's instructions (Servicebio Technology Co., Ltd., Wuhan, P. R. China). Absorbance was measured at 490 nm using a microplate reader (Bio-Rad; Hercules, CA, USA). Cell viability was calculated using Equation S3.

$$Cell\ viability\ ratio\ （\%）= \frac{A_{Sample} - A_{Blank}}{A_{Control} - A_{Blank}} \times 100\%$$

S3

The biocompatibility of hydrogels was further assessed by Calcein-AM/PI viability/cytotoxicity assay (Servicebio Technology Co., Ltd., Wuhan, P. R. China). HaCaT and L929 cells were seeded at 1.0×10^4 cells per well in 1.0 mL of complete medium in 24-well plates and cultured for 24 h. The medium was then replaced with fresh medium containing

hydrogel (400.0 μmol L^{-1}, 100.0 μL per well) or without hydrogel. After 24 h of incubation, cells were washed with PBS and stained with the Calcein-AM/PI dual-staining kit according to the manufacturer's protocol. Fluorescence images were captured using a Nikon Eclipse Ti inverted fluorescence microscope (Nikon, Tokyo, Japan).

Cytoprotective effect of hydrogels against H_2O_2 *in vitro*

HaCaT and L929 cells were plated at a density of 5.0×10^3 cells per well in 100.0 μL of complete medium in 96-well plates and incubated for 24 h. The medium was then replaced with fresh medium containing H_2O_2 (0−800.0 μmol L^{-1}). After 24 h, cell viability was assessed using the CCK-8 assay according to the manufacturer's instructions (Heyuan Liji Biotechnology Co., Ltd., Shanghai, P. R. China). Absorbance at 490 nm was measured using a microplate reader (Bio-Rad; Hercules, CA, USA), and cell viability was calculated as Equation S3.

The optimal H_2O_2 concentration was defined as the dose that maintained approximately 70% cell survival relative to the untreated controls.

Subsequently, HaCaT and L929 cells were seeded in 96-well plates under identical conditions. Cells were treated with the predetermined concentration of H_2O_2, in the presence or absence of hydrogel (400.0 μmol L^{-1}, 10.0 μL per well) and incubated for 24 h. Cell viability was then determined using the CCK-8 assay (Heyuan Liji Biotechnology Co., Ltd., Shanghai, P. R. China), with absorbance measured at 490 nm using a microplate reader (Bio-Rad; Hercules, CA, USA). Cell viability was calculated using Equation S3.

Intracellular reactive oxygen species assay

To evaluate the antioxidant capacity of hydrogels *in vitro*, intracellular ROS levels were quantified using fluorescent staining. HaCaT and L929 cells were seeded at a density of 1.0×10^4 cells per well in 1.0 mL complete medium in 24-well plates and allowed to adhere for 24 h. Cells were then treated with the predetermined concentration of H_2O_2, in the presence or absence of hydrogel (400.0 μmol L^{-1}, 100.0 μL per well). Intracellular ROS levels were detected using a DCFH-DA staining kit (Servicebio Technology Co., Ltd., Wuhan, P. R. China), and fluorescence images were captured using a Nikon Eclipse Ti inverted fluorescence microscope (Nikon, Tokyo, Japan).

Anti-apoptosis effect *in vitro*

To determine the anti-apoptotic properties of hydrogels, flow cytometry analysis was performed. HaCaT and L929 cells were seeded at a density of 1.0×10^4 cells per well in 1.0 mL of complete medium in 24-well plates and cultured for 24 h. Cells were then treated with the predetermined concentration of H_2O_2, in the presence or absence of hydrogel (400.0 μmol

L^{-1}, 100.0 μL per well). After incubation, cells were collected and stained using an Annexin V-FITC/PI apoptosis detection kit (Servicebio Technology Co., Ltd., Wuhan, P. R. China) according to the manufacturer's instructions. Samples were analyzed by flow cytometry (BD FACSCelesta, Shanghai, P. R. China).

Polarization regulation of RAW 264.7 macrophages

To evaluate the effects of hydrogels on macrophage polarization, flow cytometry was performed. RAW 264.7 macrophages were first primed with LPS (500.0 ng mL^{-1}, 12 h) to induce a pro-inflammatory M1 phenotype. After removing LPS, the cells were cultured for an additional 24 h in fresh medium with or without hydrogel (400.0 μmol L^{-1}). Cells were then collected and stained with CD80-SB645 (M1 marker) and CD206-PE (M2 marker) antibodies (Thermo Fisher Scientific, Waltham, MA, USA) following the manufacturer's instructions. Fluorescence signals were analyzed using a flow cytometer (BD FACSCelesta, Shanghai, P. R. China).

Cytokine secretion by RAW 264.7 macrophages

To evaluate the influence of hydrogel on cytokine secretion, macrophages were first polarized by LPS (500.0 ng mL^{-1}) stimulation for 12 h. The culture medium was then replaced, and the hydrogel was introduced to the cells. Culture supernatants were collected 2 h after hydrogel administration, and the levels of pro-inflammatory cytokines (IL-6 and TNF-α) were quantified using ELISA according to the manufacturer's protocol (Thermo Fisher Scientific, Waltham, MA, USA). Supernatants were harvested 12 h after hydrogel addition, and concentrations of anti-inflammatory cytokines (IL-10 and TGF-β) were measured following the manufacturer's instructions (Thermo Fisher Scientific, Waltham, MA, USA).

Hemolysis assay

To assess the hemocompatibility of hydrogels, fresh whole blood was washed with PBS and centrifuged at 3000 rpm for 5 min until the supernatant became clear. The erythrocytes were resuspended in PBS to prepare a 4.0% (*V*/*V*) cell suspension. Aliquots (400.0 μL) of the suspension were treated with hydrogel (400.0−12.5 μmol L^{-1}) or left untreated (control) and incubated at 37 °C for 2 h. After incubation, samples were centrifuged at 3000 rpm for 5 min, and 100.0 μL of the supernatant was transferred to a 96-well plate. Absorbance at 570 nm was measured using a microplate reader (Bio-Rad; Hercules, CA, USA). The hemolysis ratio was calculated as Equation S4.

$$Hemolysis\ ratio\ （\%）= \frac{A_{Sample} - A_{Blank}}{A_{Positive\ control} - A_{Blank}} \times 100\%$$

S4

The hemolytic response was recorded photographically, and supernatants were further analyzed for absorbance at 570 nm to confirm results.

Therapeutic evaluation *in vivo*

To evaluate the therapeutic efficacy of hydrogels in diabetic wound healing, a full-thickness skin defect model was established in male C57BL/6N mice (4−5 weeks, SPF; Charles River Laboratories, Beijing, P. R. China). After a 12 h fasting period, STZ (1.0%, *W*/*V*) dissolved in citrate buffer (pH 4.2−4.5) was administered intraperitoneally at a dose of 150.0 mg (kg body weight)$^{-1}$ (mg (kg BW)$^{-1}$). After seven days, tail-vein blood glucose was measured. Mice with glucose levels ≥ 16.7 mmol L^{-1} on two consecutive days were considered diabetic. Non-diabetic mice received a second identical STZ injection until the glycemic threshold was achieved. Successfully diabetic mice were randomly assigned to three groups (n = 6): (I) Control (PBS), (II) $EG_{45}Nle_{25}$, and (III) $EG_{45}Met_{25}$. For the wound model, mice were anesthetized with isoflurane, the dorsal area was shaved, and a 6.0-mm full-thickness circular wound was created using a sterile biopsy punch. A silicone splint (Inner diameter: 10.0 mm) was adhered around the wound margin to minimize contraction. Immediately afterward, 50.0 μL of the material (PBS, $EG_{45}Nle_{25}$, or $EG_{45}Met_{25}$) was injected into the wound bed. After *in situ* hydrogel formation, wounds were covered with sterile gauze and secured with elastic bandages. Wounds were photographed and re-treated on days 0, 3, 7, 10, and 14 post-injury. At the end of the treatment period, wound tissues were harvested and analyzed by hematoxylin and eosin (H&E), Masson's trichrome staining, immunofluorescence staining (IL-6, TNF-α, IL-10, and TGF-β), and immunohistochemistry (CD31 and VEGF).

***In vivo* cytotoxicity evaluation**

The systemic biocompatibility of hydrogels was evaluated by H&E staining of major organs (heart, liver, spleen, lungs, and kidneys) collected after treatment to assess potential histopathological changes.

Statistical analysis

The statistical data were represented as mean ± standard deviation (SD). Data analysis was conducted using GraphPad Prism (version 10.1.2) with Student's *t*-test. Significance levels were denoted as NS, no significant, *$P < 0.05$, **$P < 0.01$, ***$P < 0.001$, and ****$P < 0.0001$, respectively.

References

1 H. Xia, Q. Tang, Z. Chen, S. Cao, L. Wu, L. Hao, X. Hu, L. Sun, Z. Gu and H. Mao, *Bioact. Mater.*, 2026, **58**, 370−387.
2 D. Jia, S. Li, M. Jiang, Z. Lv, H. Wang and Z. Zheng, *ACS Appl. Mater. Interfaces*, 2024, **16**, 15752−15760.

3 J. Yang, X. Dong, W. Wei, K. Liu, X. Wu and H. Dai, *J. Mater. Chem. B*, 2024, **12**, 5377−5390.
4 H. Guo, H. Luo, J. Ou, J. Zheng, C. Huang, F. Liu and S. Ou, *Carbohydr. Polym.*, 2025, **348**, 122822.
5 Y. Jiang, J. Xu, L. Huang and K. Tang, *Int. J. Biol. Macromol.*, 2025, **322**, 146966.
6 D. Pranantyo, C. K. Yeo, Y. Wu, C. Fan, X. Xu, Y. S. Yip, M. I. G. Vos, S. H. Mahadevegowda, P. L. K. Lim, L. Yang, P. T. Hammond, D. I. Leavesley, N. S. Tan and M. B. Chan-Park, *Nat. Commun.*, 2024, **15**, 954.
7 M. Zheng, W. Song, P. Huang, Y. Huang, H. Lin, M. Zhang, H. He and J. Wu, *J. Control. Release*, 2024, **376**, 701−716.
8 Q. Yu, C. Shen, X. Wang, Z. Wang, L. Liu and J. Zhang, *Int. J. Nanomed.*, 2023, **18**, 563−578.
9 F. Zou, Y. Wang, T. Tang, Y. Zheng, Y. Xie, S. Zhu, H. Yang, H. Meng, X. Liu and J. Yang, *Chem. Eng. J.*, 2023, **451**, 138952.
10 S. Jia, J. Wang, X. Wang, X. Liu, S. Li, Y. Li, J. Li, J. Wang, S. Man, Z. Guo, Y. Sun, Z. Jia, L. Wang and X. Li, *Biomater. Sci.*, 2023, **11**, 7748−7758.
11 X. Lin, X. Yang, P. Li, Z. Xu, L. Zhao, C. Mu, D. Li and L. Ge, *ACS Appl. Mater. Interfaces*, 2023, **15**, 22817−22829.
12 A. Sun, D. Hu, X. He, X. Ji, T. Li, X. Wei and Z. Qian, *NPG Asia Mater.*, 2022, **14**, 86.

Table S1. Comparison of recent amino acid-based wound dressings to poly(amino acid) hydrogel.

Year	Form of wound dressing	Selection of amino acid/modified amino acid	Antioxidant capacity *in vitro*	Immunomodulatory ability	Effect *in vivo*	Reference
2026	Nanoplatform	Met	Not evaluated	M2/M1 = 32.36	98.73% (Day 14)	[1]
2024	Hydrogel	Met	~75% (MTT)	Not evaluated	93.80% (Day 14)	[2]
2024	Hydrogel	Met	~75% (DCFH-DA)	M1 decreased while M2 increased	95.43% (Day 28)	[3]
2025	Hydrogel	Cys	~100% (DCFH-DA)	Expression of CD206 (58.10%)	Not evaluated	[4]
2025	Microparticle	Cys	Not evaluated	Not evaluated	＞90% (Day 14)	[5]
2024	Hydrogel	*N*-Acetyl cysteine	Not evaluated	Not evaluated	＞95% (Day 14)	[6]
2024	Hydrogel	*N*-Acetyl cysteine	94.00% (MTT)	M1 decreased while M2 increased	~90% (Day 14)	[7]
2023	Hydrogel	*N*-Acetyl cysteine	Not evaluated	Not evaluated	99.21% (Day 14)	[8]
2023	Hydrogel	Cys	Not evaluated	M2/M1 ≈ 50%	93.80% (Day 18)	[9]
2023	Hydrogel	Cys	Not evaluated	Not evaluated	80.00% (Day 14)	[10]
2023	Hydrogel	Cys	Not evaluated	Not evaluated	~95% (Day 14)	[11]
2022	Hydrogel	Cys	~75% (MTT)	Not evaluated	~90% (Day 21)	[12]
Our work	Hydrogel	Met	121.90% (CCK8)	M2/M1 = 26.11	95.45% (Day 14)	

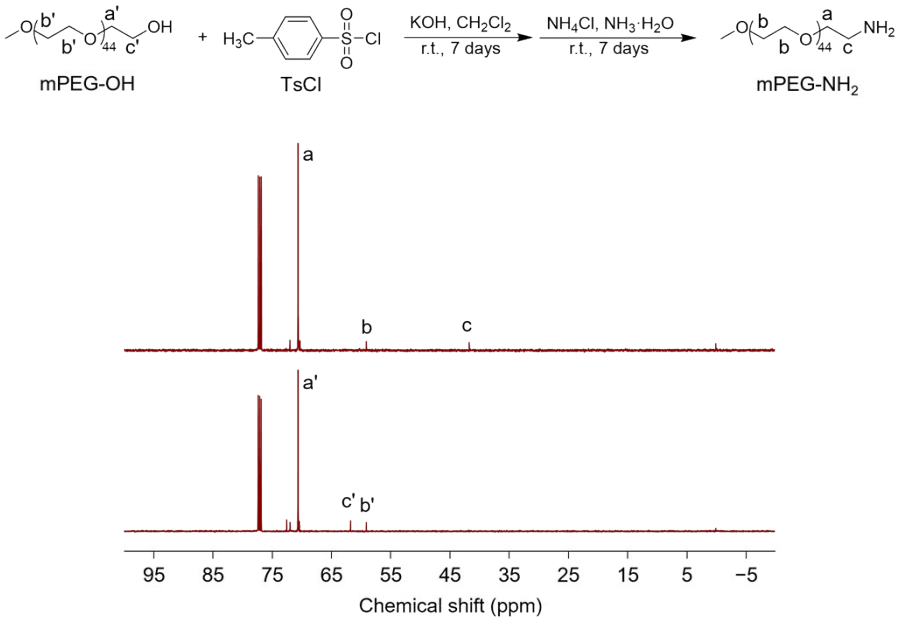

Fig. S1 ^{13}C NMR spectra of mPEG and mPEG-NH_2.

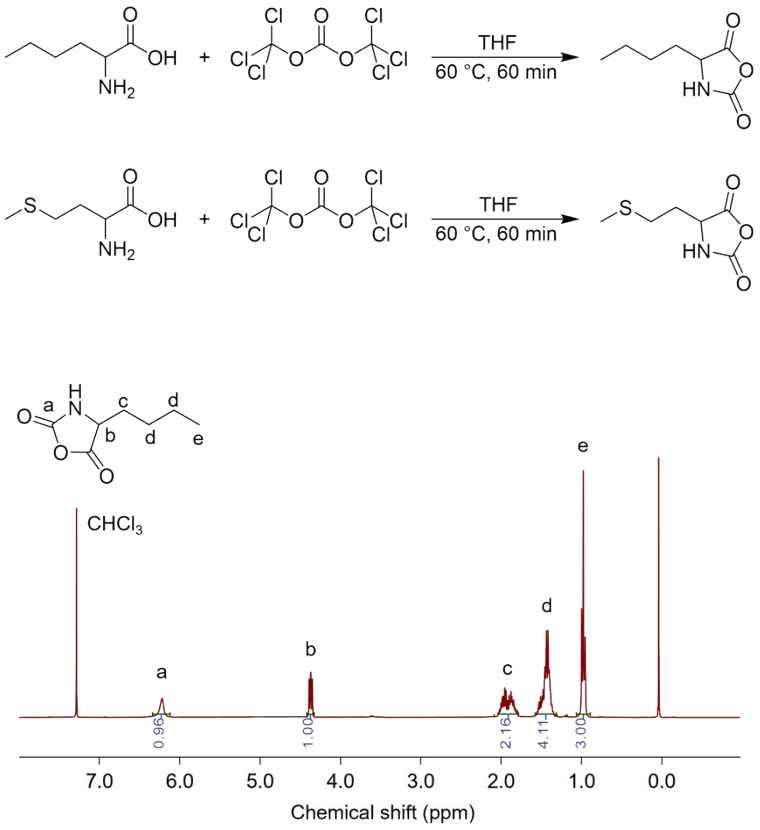

Fig. S2 ^{1}H NMR spectrum of Nle NCA.

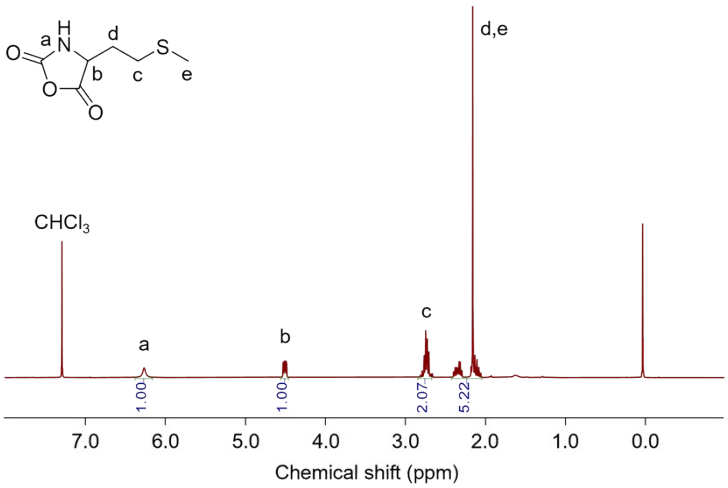

Fig. S3 ^{1}H NMR spectrum of Met NCA.

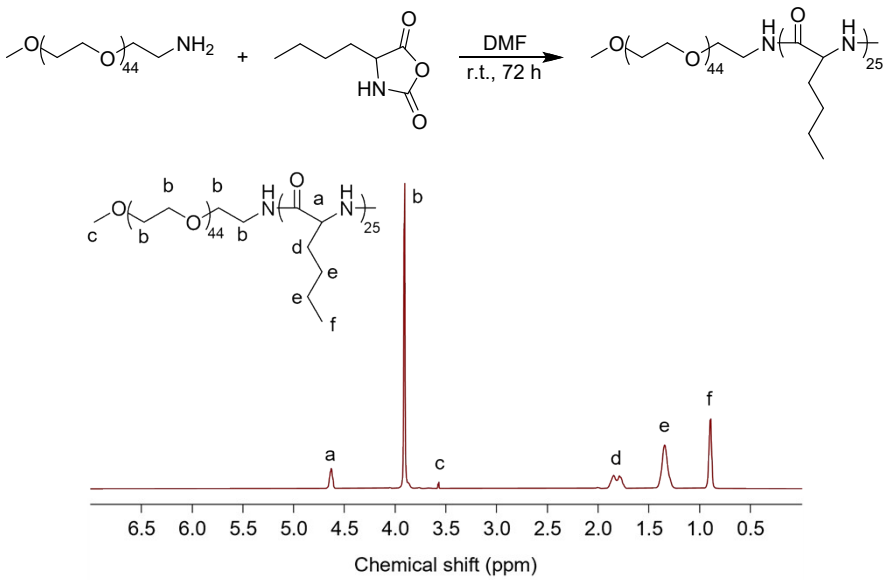

Fig. S4 ^{1}H NMR spectrum of $EG_{45}Nle_{25}$.

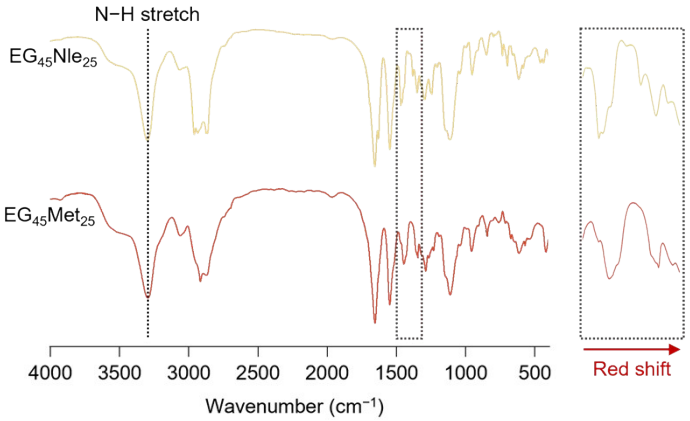

Fig. S5 FT-IR spectra of $EG_{45}Nle_{25}$ and $EG_{45}Met_{25}$.

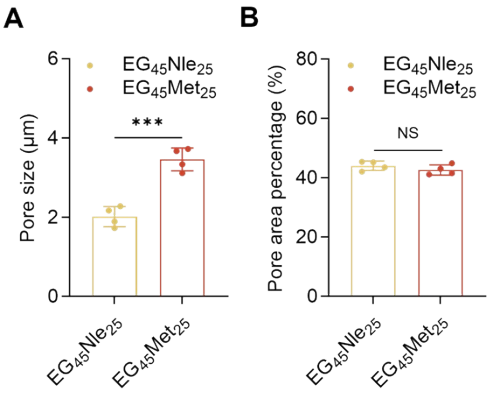

Fig. S6 Analysis results of SEM images of hydrogels. (A) Quantitative analysis of pore sizes of hydrogels. (B) Quantitative analysis of pore area percentage of hydrogels. Statistical data are represented as mean ± SD ($n = 4$; NS: no significance, ***$P < 0.001$).

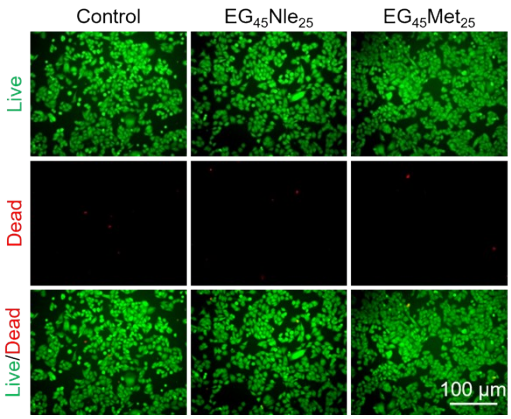

Fig. S7 Live/dead staining image of L929 cells.

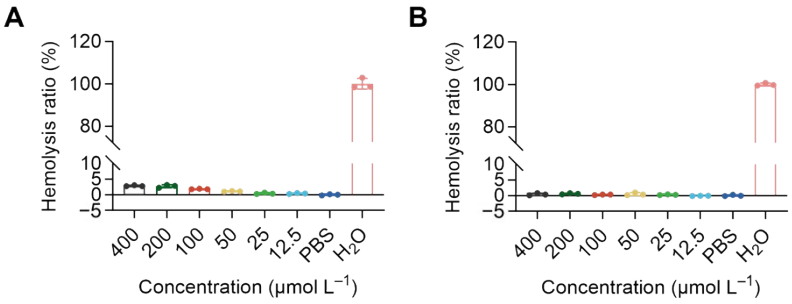

Fig. S8 Hemolytic assay of red blood cells with various (A) $EG_{45}Nle_{25}$ and (B) $EG_{45}Met_{25}$ hydrogels concentrations. Statistical data are represented as mean ± SD (n = 3).

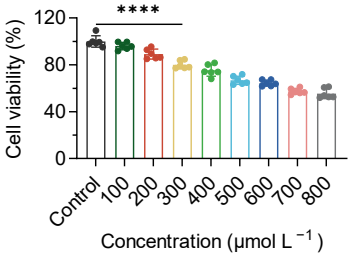

Fig. S9 Cell viability of L929 cells cultured with different concentrations of H_2O_2 for 24 h. Statistical data are represented as mean ± SD (n = 6; ****P < 0.0001).

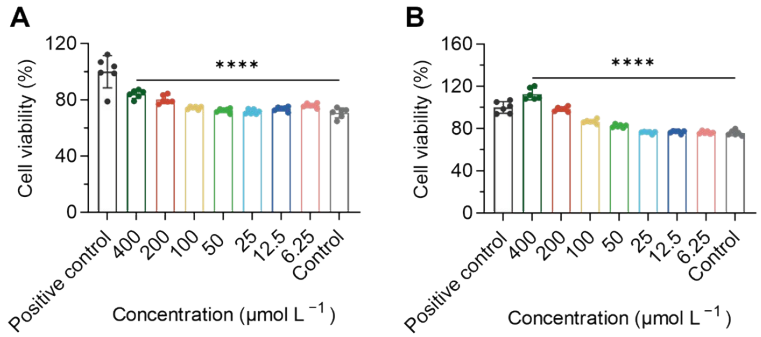

Fig. S10 Protective effects of (A) $EG_{45}Nle_{25}$ and (B) $EG_{45}Met_{25}$ hydrogels with different concentrations on L929 cells under condition of H_2O_2 for 24 h. Statistical data are represented as mean ± SD (n = 6; ****P < 0.0001).

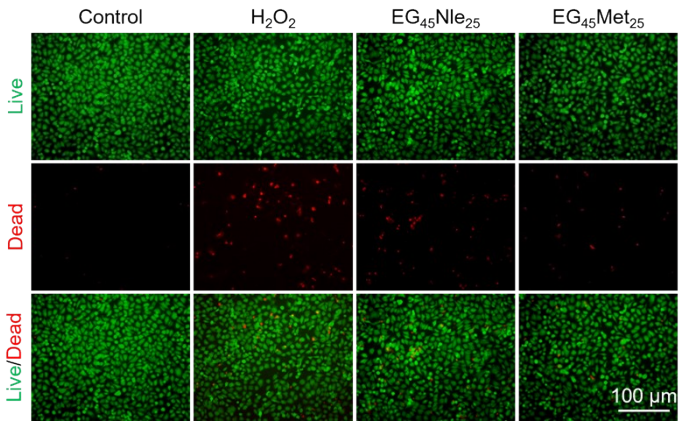

Fig. S11 Live/dead staining images of HaCaT cells under condition of H_2O_2 (600.0 μM).

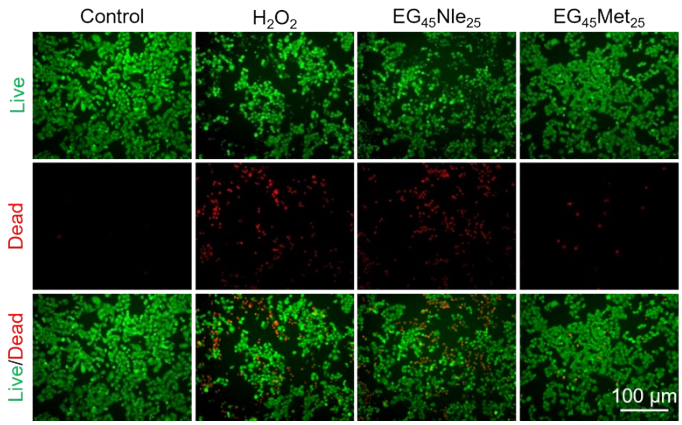

Fig. S12 Live/dead staining image of L929 cells under condition of H_2O_2 (300.0 μM).

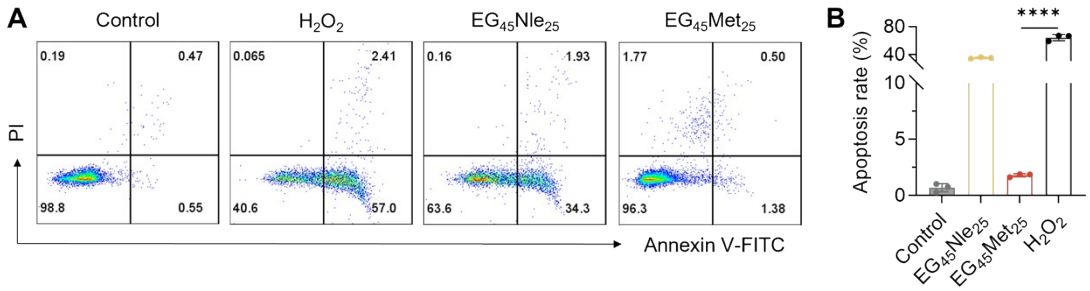

Fig. S13 Anti-apoptotic effect of hydrogels upon L929 cells under condition of H_2O_2 (300.0 μM). (A) Results of anti-apoptotic effect. (B) Quantitative analysis results. Statistical data are represented as mean ± SD ($n = 3$; ****$P < 0.0001$).

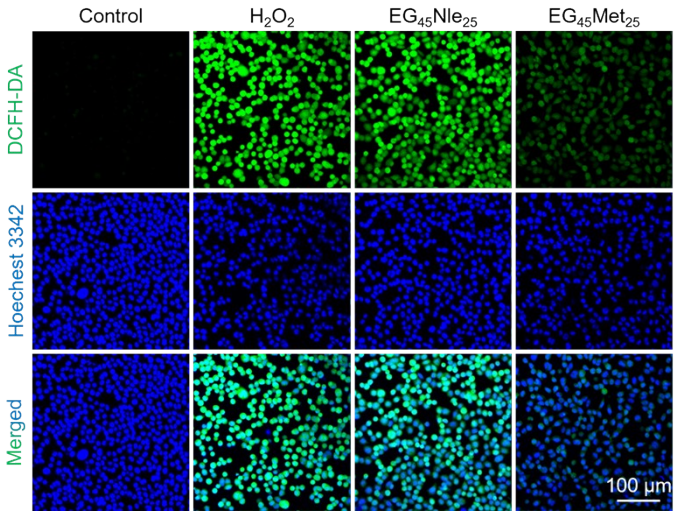

Fig. S14 ROS scavenging ability of hydrogels upon L929 cells under condition of H_2O_2 (300.0 μM).

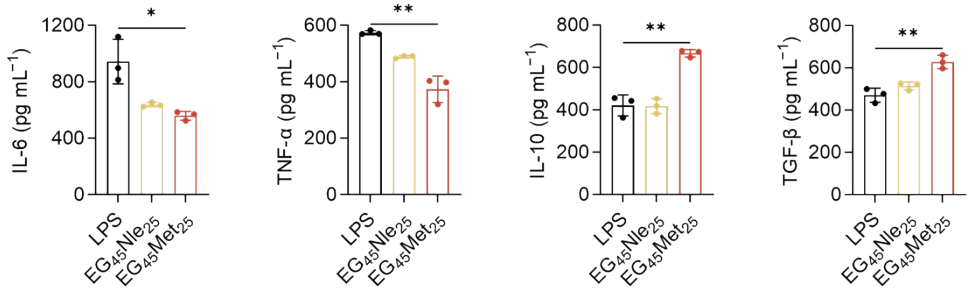

Fig. S15 Relative quantitative analysis of representative cytokines (IL-6, TNF-α, TGF-β, and IL-10) detected by ELISA. Statistical data are represented as mean ± SD (n = 3; *P < 0.05, **P < 0.01).

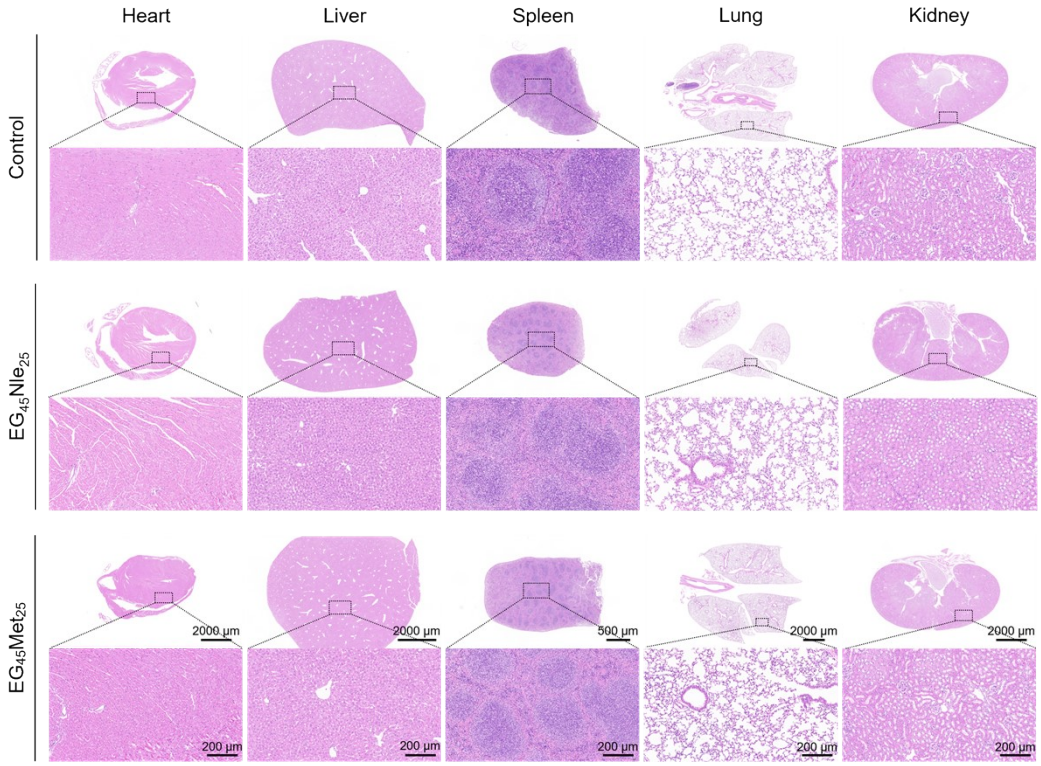

Fig. S16 Histopathological analysis of heart, liver, spleen, lung, and kidney after treatments with PBS as a Control, $EG_{45}Nle_{25}$, and $EG_{45}Met_{25}$.